

Topological phase transition in cavity optomechanical system with periodical modulation

Zhi-Xu Zhang(张志旭), Lu Qi(祁鲁), Wen-Xue Cui(崔文学), Shou Zhang(张寿), and Hong-Fu Wang(王洪福)
Citation: Chin. Phys. B, 2022, 31 (**7**): 070301. DOI: 10.1088/1674-1056/ac4a6a
Journal homepage: http://cpb.iphy.ac.cn; http://iopscience.iop.org/cpb

What follows is a list of articles you may be interested in

Real non-Hermitian energy spectra without any symmetry

Boxue Zhang(张博学), Qingya Li(李青铓), Xiao Zhang(张笑), and Ching Hua Lee(李庆华)
Chin. Phys. B, 2022, 31 (**7**): 070308. DOI: 10.1088/1674-1056/ac67c6

Geometric phase under the Unruh effect with intermediate statistics

Jun Feng(冯俊), Jing-Jun Zhang(张精俊), and Qianyi Zhang(张倩怡)
Chin. Phys. B, 2022, 31 (**5**): 050312. DOI: 10.1088/1674-1056/ac5d31

Filling up complex spectral regions through non-Hermitian disordered chains

Hui Jiang and Ching Hua Lee
Chin. Phys. B, 2022, 31 (**5**): 050307. DOI: 10.1088/1674-1056/ac4a73

Photoinduced Weyl semimetal phase and anomalous Hall effect in a three-dimensional topological insulator

Meng-Nan Chen(陈梦南) and Wen-Chao Chen(陈文潮)
Chin. Phys. B, 2021, 30 (**11**): 110308. DOI: 10.1088/1674-1056/abff29

Topological phase transitions driven by next-nearest-neighbor hopping in noncentrosymmetric cold Fermi gases

Wang Rui, Zhang Cun-Xi, Ji Qing-Shan
Chin. Phys. B, 2015, 24 (**3**): 030305. DOI: 10.1088/1674-1056/24/3/030305

Topological phase transition in cavity optomechanical system with periodical modulation

Zhi-Xu Zhang(张志旭)[1], Lu Qi(祁鲁)[2], Wen-Xue Cui(崔文学)[1,†], Shou Zhang(张寿)[1], and Hong-Fu Wang(王洪福)[1,‡]

[1] *Department of Physics, College of Science, Yanbian University, Yanji* 133002, *China*
[2] *School of Physics, Harbin Institute of Technology, Harbin* 150001, *China*

(Received 9 November 2021; revised manuscript received 21 December 2021; accepted manuscript online 12 January 2022)

We investigate the topological phase transition and the enhanced topological effect in a cavity optomechanical system with periodical modulation. By calculating the steady-state equations of the system, the steady-state conditions of cavity fields and the restricted conditions of effective optomechanical couplings are demonstrated. It is found that the cavity optomechanical system can be modulated to different topological Su–Schrieffer–Heeger (SSH) phases via designing the optomechanical couplings legitimately. Meanwhile, combining the effective optomechanical couplings and the probability distributions of gap states, we reveal the topological phase transition between trivial SSH phase and nontrivial SSH phase via adjusting the decay rates of cavity fields. Moreover, we find that the enhanced topological effect of gap states can be achieved by enlarging the size of system and adjusting the decay rates of cavity fields.

Keywords: topological phase transition; periodical modulation; enhanced topological effect

PACS: 03.65.Vf, 73.43.Nq **DOI:** 10.1088/1674-1056/ac4a6a

1. Introduction

Topological insulators and superconductors have been the theoretical and experimental subjects of recent interests in condensed matter physics.[1–5] Among them, topological insulators are known for holding robust edge states and well-defined inner products, which endows them potential for applications in quantum computing.[6] Moreover, their various extensions establish the testing ground for exploring the interplay between topological phases and non-Hermiticity.[7–11] Numerous insights into the physical meaning of topological invariant can be validated by the bulk-boundary correspondence relationship in Hermitian systems. Although flaws may exist in this correspondence relationship for non-Hermitian systems, this dilemma is handled commendably with the introduction of generalized Brillouin zone (GBZ) theory.[12–17] The great advance of topological insulator paves the way to combine the topology and other disciplines.[18–20]

Parallel to the promotion of topological phases in theory, the experimental research on topological insulator has also made delightful achievements and embodied ample discoveries.[21–26] A series of investigations related to quantum matter in macro and micro scales[27–34] broaden the research fields of topological insulator. Henceforth, the research on topological systems is well coalesced with sorts of experimental platforms, such as solid state,[35,36] cold atoms,[37–39] photonics,[40–42] optical lattices,[43–48] and even acoustics.[49,50] Among these physical systems, the cavity optomechanical system, which is composed of optical cavity fields and micro-mechanical resonators, stands out by its facility of manipulation and accuracy of results. Moreover, the multiple-cavity optomechanical system provides an excellent approach to map the topological tight-binding model and to investigate topological phase transition. For example, a feasible regime has been provided to explore Anderson localization effect in disordered cavity optomechanical arrays in Ref. [51]. The Z_2 topological insulator is simulated based on one-dimensional cavity optomechanical cells' arrays in Ref. [52]. A new approach based on the optomechanical array is investigated to map the topological non-trivial Su–Schrieffer–Heeger (SSH) model in Ref. [53]. Especially, based on the cavity fields driven by the time-dependent external driving laser, dissipation-induced topological phase transition and periodical-driving-induced state transfer have been illustrated in Ref. [54]. It is worth noting that periodic modulation of cavity fields and external driving laser are two important ways to realize the steady state of the cavity fields. These studies did not, however, delve into the approach of the periodical modulation of cavity fields. Inspired by the studies mentioned above, a question arises naturally: Is it possible to realize topological phase transition based on the periodical modulation of cavity fields rather than time-dependent external driving laser?

In this paper, we explore the topological phase transition and the enhanced topological effect under steady-state regime in a cavity optomechanical system with periodical modulation of cavity fields. Through investigating the steady-state dynam-

†Corresponding author. E-mail: cuiwenxue@ybu.edu.cn
‡Corresponding author. E-mail: hfwang@ybu.edu.cn

© 2022 Chinese Physical Society and IOP Publishing Ltd

ics of system, we obtain the steady-state solutions and the restricted conditions of effective optomechanical couplings. It is found that the cavity fields are left in periodical oscillating stable state after a long period of evolution. Under the steady-state regime and the restricted conditions, we realize the modulation of the system to different topological SSH phases via designing the optomechanical couplings legitimately. Meanwhile, in virtue of the effective optomechanical couplings and the energy spectrum as well as probability distributions for gap states, we investigate the phase transition between topological trivial SSH phase and nontrivial SSH phase via adjusting the decay rates of cavity fields. Moreover, in order to make up the unapparent topological effect of gap states under topological nontrivial SSH phase, two feasible approaches are provided to realize the enhanced topological effect of gap states.

2. Model and Hamiltonian

The cavity optomechanical system under consideration is shown in Fig. 1, which includes two resonators and two cavity fields with periodical modulation. The total Hamiltonian of the system is written as

$$\begin{aligned} H &= \sum_{n=1,2}\{[\omega_{a,n}+\Lambda_n(t)]a_n^\dagger a_n+\omega_{b,n}b_n^\dagger b_n \\ &\quad +\Omega_n a_n^\dagger \mathrm{e}^{-\mathrm{i}\omega_{d,n}t}+\Omega_n^* a_n \mathrm{e}^{\mathrm{i}\omega_{d,n}t}\} \\ &\quad -g_1(a_1^\dagger a_1-a_2^\dagger a_2)(b_1^\dagger+b_1)-g_2 a_2^\dagger a_2(b_2^\dagger+b_2), \end{aligned} \tag{1}$$

where $a_n^\dagger$ (a_n) and $b_n^\dagger$ (b_n) are the creation (annihilation) operators of the cavity fields and resonators, respectively. The first two terms represent the energy of cavity fields and resonators, in which $\omega_{a,n}$ and $\omega_{b,n}$ are the frequencies of the cavity fields and resonators, $\Lambda_n(t)$ is the modulation frequency of cavity field and the specific form is given in next section. The third and fourth terms are the energy of driving laser with amplitude Ω_n and frequency $\omega_{d,n}$. The last two terms denote the interaction Hamiltonian between cavity fields and resonators with optomechanical couplings g_1 and g_2. After applying a rotating transformation with respect to the driving frequency, the Hamiltonian is given by

$$\begin{aligned} H_1 &= \sum_{n=1,2}\left[\sigma_{a,n}a_n^\dagger a_n+\omega_{b,n}b_n^\dagger b_n+\Omega_n a_n^\dagger+\Omega_n^* a_n\right] \\ &\quad -g_1(a_1^\dagger a_1-a_2^\dagger a_2)(b_1^\dagger+b_1)-g_2 a_2^\dagger a_2(b_2^\dagger+b_2), \end{aligned} \tag{2}$$

where $\sigma_{a,n}=\Delta_{a,n}+\Lambda_n(t)$ ($\Delta_{a,n}=\omega_{a,n}-\omega_{d,n}$) represents the detuning between the cavity fields and the driving lasers. A standard linearization process is performed to determine the steady-state dynamics of the system. We rewrite the creation and annihilation operators as $a_n=\langle a_n\rangle+\delta a_n=\alpha_n+\delta a_n$ and $b_n=\langle b_n\rangle+\delta b_n=\beta_n+\delta b_n$. After dropping the notation δ for all the fluctuation operators δa_n (δb_n), the Hamiltonian can be obtained as

$$\begin{aligned} H_2 &= \sum_{n=1,2}\left[\sigma'_{a,n}a_n^\dagger a_n+\omega_{b,n}b_n^\dagger b_n\right] \\ &\quad -g_1(\alpha_1^* a_1+\alpha_1 a_1^\dagger-\alpha_2^* a_2-\alpha_2 a_2^\dagger)(b_1^\dagger+b_1) \\ &\quad -g_2(\alpha_2^* a_2+\alpha_2 a_2^\dagger)(b_2^\dagger+b_2), \end{aligned} \tag{3}$$

in which $\sigma'_{a,1}=\sigma_{a,1}-g_1(\beta_1^*+\beta_1)$ and $\sigma'_{a,2}=\sigma_{a,2}+g_1(\beta_1^*+\beta_1)-g_2(\beta_2^*+\beta_2)$ are the effective cavity field detuning. Under the red-detuning regime, the counter rotating wave terms can be dropped safely and the final effective Hamiltonian can be written as

$$H_{\mathrm{eff}}=\left[-G_1 a_1^\dagger b_1+G_2 a_2^\dagger b_1-G_3 a_2^\dagger b_2\right]+\mathrm{H.c.}, \tag{4}$$

where $G_1=g_1\alpha_1$, $G_2=g_1\alpha_2$, and $G_3=g_2\alpha_2$ are effective optomechanical couplings. We find that there are only the nearest neighbor interactions between cavity fields and resonators in Eq. (4), which hold the same form with the topological tight-binding Hamiltonian. This means that an equivalence relation can be set up between the cavity optomechanical system and the topological system via legitimately designing the optomechanical couplings. According to the Floquet theory, the cavity field amplitude α_n and resonator amplitude β_n will obtain the same oscillating period with time-dependent modulation of cavity fields after a long time gradual evolution. We stress that the periodical modulation of cavity fields leaves the steady-state dynamics of the system to be time-dependent and the details are discussed in the following.

3. Steady-state conditions of cavity fields and the restricted conditions of effective optomechanical couplings

Here, we consider the periodically time-dependent modulations of cavity fields with $\Lambda_1(t)=\lambda_1\nu_1\cos 2\pi\nu_1 t$ and $\Lambda_2(t)=\lambda_2\nu_2\cos 2\pi\nu_2 t$. The approachable technique to realize the frequency modulations of the cavity fields has been proposed in Ref. [55] via a laser irradiated onto the cavity field and discussed in Refs. [56,57]. Significantly, this is different in nature between our work and Ref. [54], in which the time-dependent external driving laser is considered to realize topological phase transition rather than time-dependent modulations of cavity fields. In this way, the dynamics of cavity fields are determined by the following steady-state equations (see the appendix for details) with

$$\begin{aligned} \dot{\alpha_1} &= -\mathrm{i}[\sigma_{a,1}-g_1(\beta_1^*+\beta_1)]\alpha_1-\mathrm{i}\Omega_1-\frac{\kappa_1}{2}\alpha_1, \\ \dot{\alpha_2} &= -\mathrm{i}[\sigma_{a,2}+g_1(\beta_1^*+\beta_1)-g_2(\beta_2^*+\beta_2)]\alpha_2-\mathrm{i}\Omega_2-\frac{\kappa_2}{2}\alpha_2, \\ \dot{\beta_1} &= -\mathrm{i}[\omega_{b,1}\beta_1-g_1(|\alpha_1|^2-|\alpha_2|^2)]-\frac{\gamma_1}{2}\beta_1, \\ \dot{\beta_2} &= -\mathrm{i}(\omega_{b,2}\beta_2-g_2|\alpha_2|^2)-\frac{\gamma_2}{2}\beta_2, \end{aligned} \tag{5}$$

where κ_j and γ_j (with $j = 1,2$) are the decay rates of the cavity fields and the damping rates of the resonators, respectively. The steady-state equations indicate that the cavity fields α_1 and α_2 leave to be time-dependent stable state due to the existence of the periodically modulation of $\Lambda_1(t)$ and $\Lambda_2(t)$, when the system undergoes a long period of evolution. To explore the topological properties, we principally concentrate on how the final periodically time-dependent steady-state cavity fields affect the effective optomechanical couplings and the topology of the system model. As mentioned above, the final stable states are influenced by the periodical modulation of the cavity fields, which further determines the effective optomechanical couplings. Therefore, a decisive procedure of simulating topological structure and investigating topological properties is to leave the system in the stable state.

To illustrate this further, we give a visual interpretation of how the cavity optomechanical system is modulated into different topological phases under steady-state conditions. The key parameters in the present system are determined as $g_1 = g_2$, $\lambda_1 = \lambda_2$, $\nu_1 = \nu_2$, and $\kappa_1 = \kappa_2$. The dynamics of cavity fields are given in Figs. 2(a) and 2(b), in which the cavity fields' amplitudes α_1 and α_2 are both left in a periodic oscillating stable state due to the periodically time-dependent modulation of cavity fields. Moreover, we find that the steady-state cavity fields amplitudes satisfy $|\alpha_1| < |\alpha_2|$, indicating the effective optomechanical couplings $|-g_1\alpha_1| < |g_1\alpha_2| > |-g_2\alpha_2|$ ($|-G_1| < |G_2| > |-G_3|$). This result can also be verified in Fig. 2(c), in which the ratio of steady-state cavity fields' amplitudes $|\alpha_1|/|\alpha_2|$ is less than 1. This phenomenon originates in the structure of our model shown in Fig. 1, in which the cavity a_1 only couples one resonator b_1 in comparison to cavity a_2 coupled two resonators b_1 and b_2 simultaneously. Interestingly, in virtue of the above phenomenon, we find that the effective optomechanical couplings in Eq. (4) can be artificially controlled by suitably altering optomechanical couplings g_n and steady-state cavity fields α_n, which indicates that we can modulate the cavity optomechanical system to different topological phases if we regard the cavity and resonator as a diatomic cell (i.e., a_1 (a_2) and b_1 (b_2) as a cell). Significantly, in order to realize a perfect correspondence, we have to guarantee a criterion of $|-G_1| \approx |-G_3|$ ($|-g_1\alpha_1| \approx |-g_2\alpha_2|$). The reason why this approximate equivalence holds is that adding disorder without breaking the symmetry will not influence the topology of system. To be convincing, we give two examples to detailedly show that the proposed system can not only be modulated to topological trivial and nontrivial SSH phases but also undergo a topological phase transition via adjusting the system parameter in the next section.

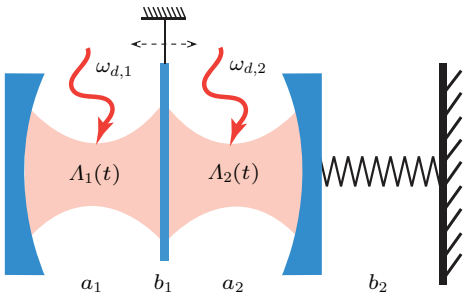


Fig. 1. Schematic diagram of the considered cavity optomechanical system. The resonators b_1 and b_2 are connected with cavity fields a_1 and a_2, which are periodically modulated by $\Lambda_1(t)$ and $\Lambda_2(t)$, respectively. The cavity field α_1 (α_2) is driven by an external laser with driving amplitude Ω_1 (Ω_2) and driving frequency $\omega_{d,1}$ ($\omega_{d,2}$). The damping rate of resonator b_1 (b_2) and the decay rate of cavity field a_1 (a_2) are γ_1 (γ_2) and κ_1 (κ_2), respectively.

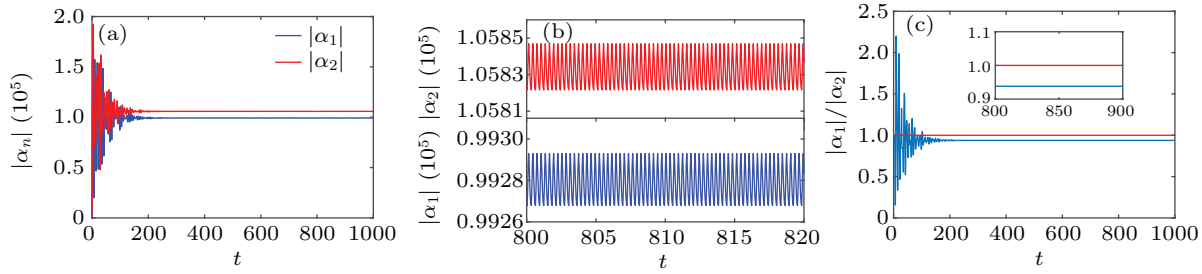


Fig. 2. The steady-state cavity fields versus time t. (a) The dynamics evolution of cavity fields α_1 and α_2. (b) The steady-state dynamics of cavity fields α_1 and α_2. (c) The ratio between the steady-state cavity field amplitudes α_1 and α_2. The red line denotes $|\alpha_1|/|\alpha_2| = 1$. In (a)–(c), the parameters are taken as $\omega_{b,1} = \omega_{b,2} = \omega_b$ (set ω_b as the energy unit), $\nu_1 = \nu_2 = 1 \times 10\omega_b$, $\Delta_{a,1} = \Delta_{a,2} = \omega_b$, $g_1 = g_2 = 1.5 \times 10^{-6}\omega_b$, $\Omega_1 = \Omega_2 = 1 \times 10^5\omega_b$, $\kappa_1 = \kappa_2 = 0.1\omega_b$, $\lambda_1 = \lambda_2 = 1 \times 10^{-2}\omega_b$ and $\gamma_1 = \gamma_2 = 1 \times 10^{-5}\omega_b$.

4. Topological phase transition induced by cavity field parameters

Firstly, we take $g_1 < g_2$ into consideration. To explore the steady-state dynamic of system, we demonstrate the steady-state cavity fields in Fig. 3(a) with $g_1 = 1.0 \times 10^{-6}\omega_b$ and $g_2 = 5.0 \times 10^{-6}\omega_b$, in which the cavity fields α_1 and α_2 are both left in periodical oscillating stable state after a long time evolution and this phenomenon is contributed to the periodical modulation of cavity fields. We also find that the final cavity filed amplitude $|\alpha_1|$ is larger than $|\alpha_2|$ when both the cavity fields reach stable state. In addition, the cavity field α_2 has oscillation width smaller than cavity field α_1, whose reason is that the decay rate of cavity field α_2 is much larger than that of cavity field α_1. Combining the above results, we find that the steady-state cavity fields and the optomechanical couplings

satisfy $|\alpha_1| > |\alpha_2|$ and $|g_1| < |g_2|$, which further indicates that $|-g_1\alpha_1| > |g_1\alpha_2| < |-g_2\alpha_2|$ ($|-G_1| > |G_2| < |-G_3|$). Significantly, another required restriction is that the first effective optomechanical coupling must be equal to the third one. To ensure this restriction, we plot the ratio between the first and the third effective optomechanical coupling, as shown in Fig. 3(b), in which $|G_1|/|G_3| \approx 1$ when the cavity fields reach stable state. The above results reveal that the effective optomechanical couplings satisfy $|-G_1|$ ($|-G_3|$) $> |G_2|$ and $|G_1| \approx |G_3|$, which signifies that the intra-cell coupling is larger than the inter-cell one and the system is left in topological trivial SSH phase.

Then, with a similar process, we analyze the case of $g_1 > g_2$. Analogously, when the optomechanical couplings $g_1 = 1.61 \times 10^{-6}\omega_b$ and $g_2 = 1.51 \times 10^{-6}\omega_b$, we show the steady-state dynamics of cavity fields in Fig. 3(c), in which the two cavity fields α_1 and α_2 are both left in periodical oscillating stable state and the final steady-state amplitude of cavity filed $|\alpha_1|$ is smaller than $|\alpha_2|$ in the illustration. Here, different from the previous case, we find that the steady-state cavity fields and the optomechanical couplings guarantee $|\alpha_1| < |\alpha_2|$ and $|g_1| > |g_2|$, which also manifests $|-g_1\alpha_1| < |g_1\alpha_2| > |-g_2\alpha_2|$ ($|-G_1| < |G_2| > |-G_3|$). Of course, we should also ensure that the first effective optomechanical coupling equals the third one and the result is shown in Fig. 3(d), in which $|G_1|/|G_3| \approx 1$ when the system reaches in stable state. By analyzing effective optomechanical couplings, it is found that the intra-cell coupling strength is smaller than the inter-cell one and the present cavity optomechanical system is left in topological nontrivial SSH phase.

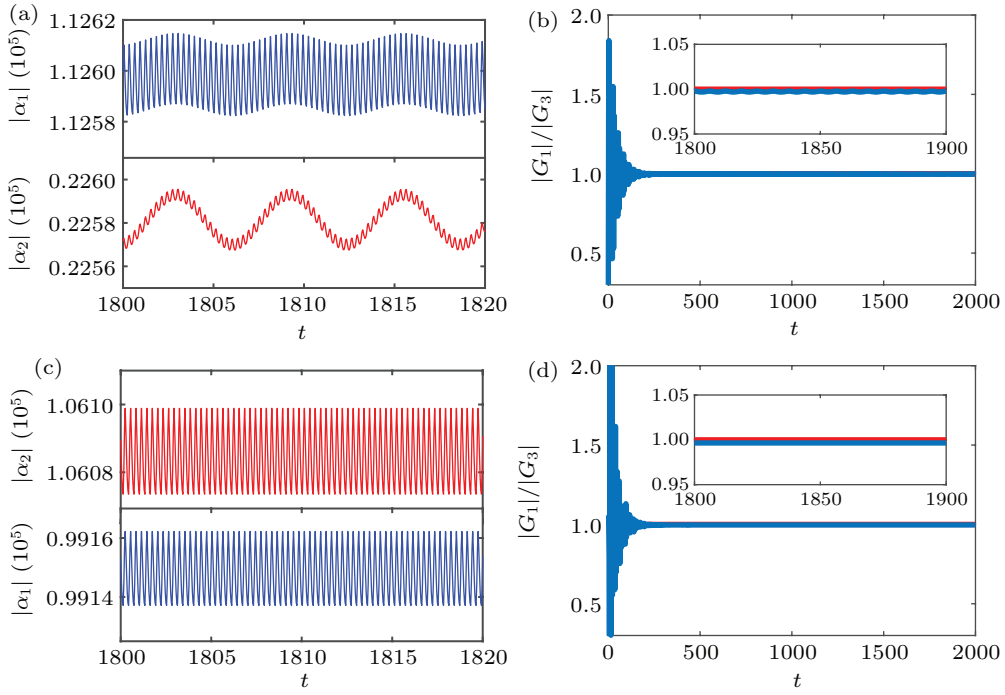


Fig. 3. The steady-state dynamics of system. (a) The steady-state dynamics and (b) the ratio of effective optomechanical coupling for final steady-state of cavity fields with topological trivial SSH phase versus time t, in which $g_1 = 1.0 \times 10^{-6}\omega_b$, $g_2 = 5.0 \times 10^{-6}\omega_b$, and $\kappa_1 = 0.1\omega_b$, $\kappa_2 = 8.63\omega_b$. (c) The steady-state dynamics and (d) the ratio of effective optomechanical couplings for final steady-state cavity fields with topological nontrivial SSH phase versus time t, in which $g_1 = 1.61 \times 10^{-6}\omega_b$, $g_2 = 1.51 \times 10^{-6}\omega_b$, $\kappa_1 = 0.1\omega_b$, and $\kappa_2 = 0.9\omega_b$.

For the sake of further insight, in Fig. 4 we show the energy spectrum and the probability distributions of gap states corresponding to the cases in Fig. 3. With the same parameters as given in Figs. 3(a)–3(b), we demonstrate the energy spectra in Fig. 4(a), in which the blue and red lines represent gap states, the green lines denote bulk states. We find that the gap states tightly stick to bulk states, meaning that the gap states merge into bulk states and no localized edge states appear. Moreover, the probability distribution for one of the gap states is shown in Fig. 4(b), in which they have almost the same probability distribution at each lattice site (around 0.25), which indicates that all the states are extended and they possess the same probability at each site. Combining the energy spectra and probability distributions of gap states, we find that the system is left in topological trivial SSH phase under this parameter regime. Moreover, the numerical results in Figs. 4(a)–4(b) are identified with the analysis of effective optomechanical couplings in Fig. 3(a), which further indicates that the proposed system is modulated to topological trivial SSH phase.

Furthermore, we also depict the energy spectra in Fig. 4(c) with the same parameters as in Figs. 3(c)–3(d), in which the two gap states are isolated from the bulk states. In addition, the probability distribution for one of the gap states is shown in Fig. 4(d), in which the probability distribution reaches around 0.34 for edge sites and 0.16 for the second

and third sites, indicating that the localized edge states appear and they have the maximal distributions at the end of lattice. Through analyzing the energy spectra and probability distributions of gap states, we find that the system is left in topological nontrivial SSH phase under this parameter regime. One can clearly see that the numerical results in Figs. 4(c)–4(d) are in accord with the analysis of the effective optomechanical couplings in Fig. 3(c), which indicates that the system is modulated to topological nontrivial SSH phase. However, there is a little regret, the localized effect of gap states is not very obvious for nontrivial SSH phase. The reason lies in that the difference between $|G_1|$ and $|G_2|$ is small, though the effective optomechanical couplings satisfy $|G_1| \approx |G_3| > |G_2|$, which induces the unapparent localized effect of edge states and this small flaw will be dealt with in the next section.

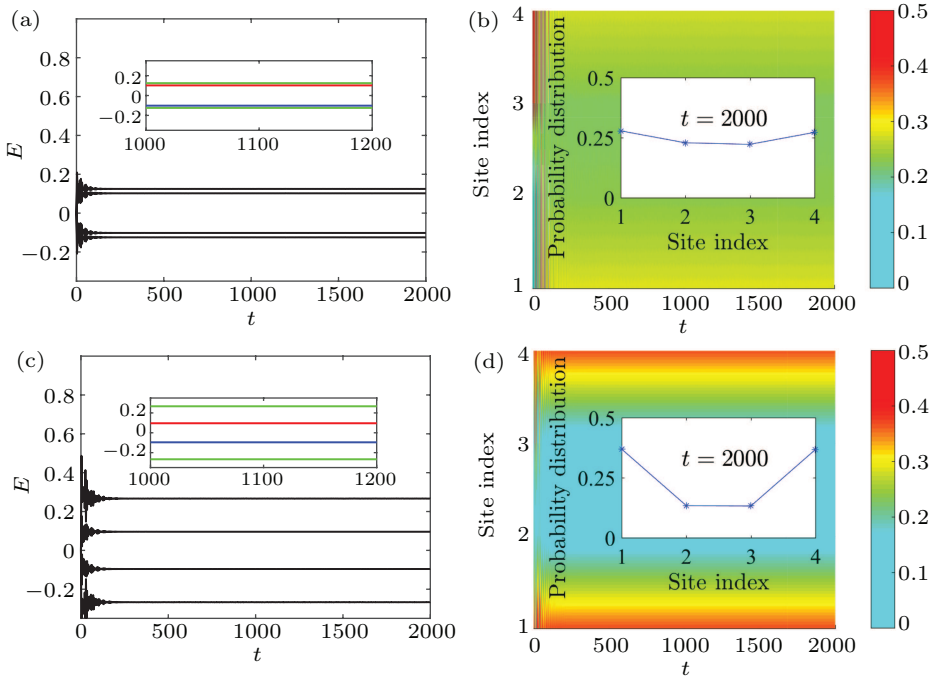


Fig. 4. The energy spectrum and probability distributions (i.e., the square of module of eigenstates at a given time) of gap states of the system. (a) The energy spectrum and (b) probability distributions of gap states with trivial SSH phase versus time t, in which the parameters are the same as those in Figs. 3(a) and 3(b). (c) The energy spectrum and (d) probability distributions for gap states with nontrivial SSH phase versus time t, in which the parameters are the same as those in Figs. 3(c) and 3(d).

Combining the above analysis, we can draw a conclusion that we can realize the topological phase transition from topological trivial SSH phase to nontrivial SSH phase by designing the optomechanical coupling g_1 (g_2) and adjusting the decay rates of cavity fields κ_1 (κ_2) appropriately. Meanwhile, the analysis of the effective optomechanical couplings is closely related to the results of the probability distributions of gap states. Compared with Ref. [54], our work realizes the topological phase transition based on periodical modulation of cavity fields instead of time-dependent external driving laser and provides a new approach to explore the topological phase of matters.

5. Enhanced topological effect

From the previous discussion, we find that the gap states under topological nontrivial SSH phase shows unapparent localized effect. In addition to the theoretical analysis, we also provide the corresponding solutions to handle the deficiency. In order to realize the enhanced topological effect of gap states, it needs to ensure that there is a huge difference between the intra-cell and inter-cell coupling strengths, which means that the effective optomechanical coupling should guarantee $|-G_1| \approx |-G_3| \ll |G_2|$. This relationship requires that the first cavity field has less import or greater decay rate than the second cavity field. Based on the above analysis, we provide a feasible regime to realize the enhanced topological effect of gap states, as shown in Fig. 5, where the decay rate of the first cavity field is much larger than the second one. In Fig. 5(a), we plot the dynamics of two steady-state cavity fields with $\kappa_1 = 2.95\omega_b$ and $\kappa_2 = 0.1\omega_b$, in which we find that the final steady-state cavity fields satisfy $|\alpha_2| \gg |\alpha_1|$ compared with the result in Fig. 3(c). Additionally, the cavity field α_1 has smaller oscillation width than cavity field α_2, whose reason lies in that the decay rate κ_1 is much larger than κ_2. Here, $g_1 = 2.0 \times 10^{-6}\omega_b$ and $g_2 = 1.0 \times 10^{-6}\omega_b$, indicating that $|-g_1\alpha_1| < |g_1\alpha_2| > |-g_2\alpha_2|$. Significantly, to ensure the restricted conditions, the relationship of effective optomechanical coupling $|G_1|/|G_3| \approx 1$ should also be guaranteed and the result is shown in Fig. 5(b). Moreover, we depict the spectrum and probability distribution for gap state in Figs. 5(c)

and 5(d), respectively. In Fig. 5(c), we find that the two gap states are isolated from bulk, meaning that the edge states appear and localize at the boundary of the lattice system. This result can be obviously observed in Fig. 5(d), in which the localized effect of gap state is greatly enhanced and the distributions of edge states reach around 0.43 at edge sites, which is larger than the corresponding results 0.34 in Fig. 4(d). This phenomenon reveals that magnifying the decay rates of cavity fields is approachable to realize the enhanced localized effect of gap states.

Then, we show that enlarging the size of system can also enhance the localized effect. The original reason derives from that the edge state is exponentially localized for the topological nontrivial SSH model with large enough size of system.[13,58] While the size of the system is small, the exponentially localized effect is not obvious. Therefore, enlarging the size of system is an approachable way to realize the enhanced localized effect of gap states. However, large size of system puts new requirements for the proposed system. For example, for a cavity optomechanical system with N cells, there are $2N-1$ effective optomechanical couplings. To ensure the restricted conditions, we must guarantee that the even effective optomechanical couplings are equal, and the same conditions for odd ones, i.e., $G_1 = G_3 = \cdots = G_{2N-1}$ and $G_2 = G_4 = \cdots = G_{2N-2}$. Moreover, the effective optomechanical coupling should satisfy $G_i < G_j$, with i and j denoting odd number and even number, respectively. Correspondingly, the steady-state cavity fields and the optomechanical couplings need to satisfy $|\alpha_N| > |\alpha_{N-1}| > |\alpha_{N-2}| > \cdots > |\alpha_1|$ and $g_1 > g_2 > g_3 > \cdots > g_N$. Furthermore, the decay rates of cavity fields are required to satisfy $\kappa_1 > \kappa_2 > \kappa_3 > \cdots > \kappa_N$ for the topological nontrivial case. Similar to the previous case, modulating topological trivial SSH phase with N cells is also feasible, the difference is that the effective optomechanical coupling should satisfy $G_i > G_j$. This requires $|\alpha_1| > |\alpha_2| > |\alpha_3| > \cdots > |\alpha_N|$ and $g_N > g_{N-1} > g_{N-2} > \cdots > g_1$. By this means, the present system can be extended to larger size for topological trivial and nontrivial SSH phases, which also indicates that enlarging the size of system is a feasible approach to reduce the size effect and to enhance the localized effect of gap states.

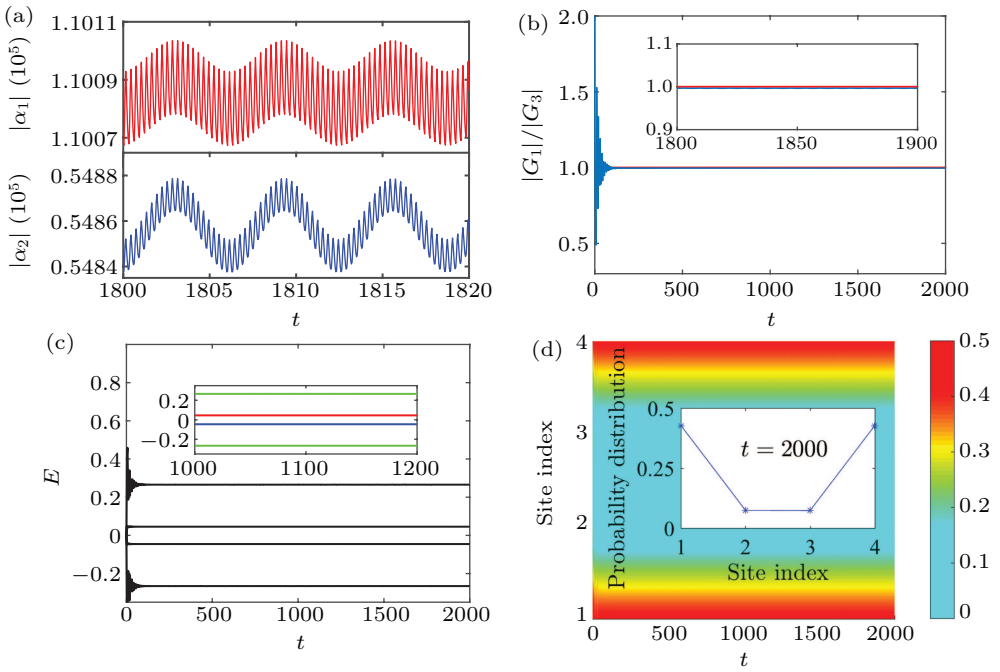


Fig. 5. The steady-state dynamics of system when $\kappa_1 \gg \kappa_2$. (a) The stead-state cavity fields α_1 and α_2 versus time t, respectively. (b) The ratio between the effective optomechanical couplings G_1 and G_3. (c) The energy spectrum of system with topological nontrivial SSH phase. (d) The probability distribution of gap states in (c), in which the gap states exhibit larger distribution at the ends of the system. The parameters are chosen as $g_1 = 2.0 \times 10^{-6}\omega_b$, $g_2 = 1.0 \times 10^{-6}\omega_b$, $\kappa_1 = 2.95\omega_b$, and $\kappa_2 = 0.1\omega_b$. The other parameters are the same as those in Figs. 3(c) and 3(d).

6. Conclusions

In summary, we have investigated the phase transition between topological trivial SSH phase and nontrivial SSH phase in a cavity optomechanical system with periodical modulation. Through calculating the steady-state dynamics, we obtain the steady-state solutions of system and provide the restricted conditions of the effective optomechanical couplings. It is found that the final cavity fields are left in periodical oscillating stable state after a long period of evolution. Under the steady-state regime and the restricted conditions, the proposed system can be modulated to topological trivial SSH phase and nontrivial SSH phase. Meanwhile, combining the effective optomechanical couplings and the probability distributions of gap states, we investigate the phase transition between trivial SSH phase and nontrivial SSH phase via adjusting the decay

rates of cavity fields and designing the optomechanical couplings legitimately. Moreover, in order to make up the unapparent localized effect of gap states under topological nontrivial SSH phase, we propose to realize the enhanced topological effect of gap states by enlarging the size of system and adjusting the decay rates of cavity fields.

Appendix A: The solutions of the steady-state equations

In this Appendix, we give the solutions of steady-state equations to determine the dynamics of cavity fields. The Hamiltonian after rotating transformation with respect to the driving frequency is expressed as

$$\begin{aligned} H_1 = &\sum_{n=1,2}\left[\sigma_{a,n}a_n^\dagger a_n+\omega_{b,n}b_n^\dagger b_n+\Omega_n a_n^\dagger+\Omega_n^* a_n\right] \\ &-g_1(a_1^\dagger a_1-a_2^\dagger a_2)(b_1^\dagger+b_1)-g_2 a_2^\dagger a_2(b_2^\dagger+b_2), \end{aligned} \tag{A1}$$

where $\sigma_{a,n}=\omega_{a,n}+\Lambda_n(t)-\omega_{d,n}$. One can actually determine the steady-state dynamics of system with the following form:

$$\dot{C}=\frac{\mathrm{i}}{\hbar}[\mathcal{H},C]-\frac{\mathcal{K}}{2}, \tag{A2}$$

in which $\mathcal{H}$ and $\mathcal{K}$ represent the Hamiltonian of system and the decay rates of the cavity fields (the damping rates of the resonators), respectively. In virtue of Eq. (A2), one can obtain the steady-state equations for cavity fields and resonators in the present system as follows:

$$\begin{aligned} \dot{a}_1 &= -\frac{\mathrm{i}}{\hbar}\left[\sigma_{a,1}a_1-g_1a_1(b_1^\dagger+b_1)\right]-\mathrm{i}\Omega_1-\frac{\kappa_1}{2}a_1, \\ \dot{a}_2 &= -\frac{\mathrm{i}}{\hbar}\left[\sigma_{a,2}a_2+g_1a_2(b_1^\dagger+b_1)-g_2a_2(b_2^\dagger+b_2)\right] \\ &\quad -\mathrm{i}\Omega_2-\frac{\kappa_2}{2}a_2, \\ \dot{b}_1 &= -\frac{\mathrm{i}}{\hbar}\left[w_{b,1}b_1-g_1\left(a_1^\dagger a_1-a_2^\dagger a_2\right)\right]-\frac{\gamma_1}{2}b_1, \\ \dot{b}_2 &= -\frac{\mathrm{i}}{\hbar}\left[w_{b,2}b_2-g_2a_2^\dagger a_2\right]-\frac{\gamma_2}{2}b_2. \end{aligned} \tag{A3}$$

Generally, the above nonlinear equations are difficult to be solved directly. For simplicity, we define a linearization process as $a_j=\langle a_j\rangle+\delta a_j=\alpha_j+\delta a_j$ and $b_j=\langle b_j\rangle+\delta b_j=\beta_j+\delta b_j$ $(j=1,2)$, in which $\langle a_j\rangle$ ($\langle b_j\rangle$) and δa_j (δb_j) denotes the mean value and fluctuation for cavity fields (resonators). Substituting the linear terms into Eq. (A3), the standard linearization techniques can be applied to the nonlinear equations. Then, we can obtain (here $\hbar=1$)

$$\begin{aligned} \dot{a}_1 = &-\mathrm{i}[\sigma_{a,1}\alpha_1-g_1\alpha_1(\beta_1^*+\beta_1)]-\mathrm{i}\Omega_1-\frac{\kappa_1}{2}\alpha_1 \\ &-\mathrm{i}[\sigma_{a,1}\delta a_1-g_1\alpha_1(\delta b_1+\delta b_1^\dagger)-g_1\delta a_1(\beta_1^*+\beta_1) \\ &-g_1\delta a_1(\delta b_1+\delta b_1^\dagger)]-\frac{\kappa_1}{2}\delta a_1, \\ \dot{a}_2 = &-\mathrm{i}[\sigma_{a,2}\alpha_2+g_1\alpha_2(\beta_1^*+\beta_1)-g_2\alpha_2(\beta_2^*+\beta_2)]-\mathrm{i}\Omega_2 \\ &-\mathrm{i}[\sigma_{a,2}\delta a_2+g_1\alpha_2(\delta b_1+\delta b_1^\dagger)+g_1\delta a_2(\delta b_1+\delta b_1^\dagger) \\ &+g_1\delta a_2(\beta_1^*+\beta_1)-g_2\alpha_2(\delta b_2+\delta b_2^\dagger)-\frac{\kappa_2}{2}\delta a_2 \\ &-g_2\delta a_2(\delta b_2+\delta b_2^\dagger)-g_2\delta a_2(\beta_2^*+\beta_2)]-\frac{\kappa_2}{2}\alpha_2, \\ \dot{b}_1 = &-\mathrm{i}[\omega_{b,1}\beta_1-g_1(|\alpha_1|^2-|\alpha_2|^2)]-\frac{\gamma_1}{2}\beta_1 \\ &-\mathrm{i}[\omega_{b,1}\delta b_1-g_1(\alpha_1^*\delta a_1+\alpha_1\delta a_1^\dagger+\delta a_1^\dagger\delta a_1 \\ &-\alpha_2^*\delta a_2-\alpha_2\delta a_2^\dagger-\delta a_2^\dagger\delta a_2)]-\frac{\gamma_1}{2}\delta b_1, \\ \dot{b}_2 = &-\mathrm{i}(\omega_{b,2}\beta_2-g_2|\alpha_2|^2)-\frac{\gamma_2}{2}\beta_2 \\ &-\mathrm{i}(\omega_{b,2}\delta b_2-g_2\alpha_2^*\delta a_2-g_2\alpha_2\delta a_2^\dagger)-\frac{\gamma_2}{2}\delta b_2. \end{aligned} \tag{A4}$$

After dropping the non-linearization terms, we can obtain the set of solutions for mean value operators as

$$\begin{aligned} \dot{\alpha}_1 &= -\mathrm{i}[\sigma_{a,1}\alpha_1-g_1\alpha_1(\beta_1^*+\beta_1)]-\mathrm{i}\Omega_1-\frac{\kappa_1}{2}\alpha_1, \\ \dot{\alpha}_2 &= -\mathrm{i}[\sigma_{a,2}\alpha_2+g_1\alpha_2(\beta_1^*+\beta_1)-g_2\alpha_2(\beta_2^*+\beta_2)] \\ &\quad -\mathrm{i}\Omega_2-\frac{\kappa_2}{2}\alpha_2, \\ \dot{\beta}_1 &= -\mathrm{i}[\omega_{b,1}\beta_1-g_1(|\alpha_1|^2-|\alpha_2|^2)]-\frac{\gamma_1}{2}\beta_1, \\ \dot{\beta}_2 &= -\mathrm{i}[\omega_{b,2}\beta_2-g_2|\alpha_2|^2]-\frac{\gamma_2}{2}\beta_2. \end{aligned} \tag{A5}$$

The set of solutions for quantum fluctuation operators are

$$\begin{aligned} \delta\dot{a}_1 &= -\mathrm{i}[\sigma_{a,1}\delta a_1-g_1\alpha_1(\delta b_1+\delta b_1^\dagger)]-\frac{\kappa_1}{2}\delta a_1, \\ \delta\dot{a}_2 &= -\mathrm{i}[\sigma_{a,2}\delta a_2+g_1\alpha_2(\delta b_1+\delta b_1^\dagger)-g_2\alpha_2(\delta b_2+\delta b_2^\dagger)] \\ &\quad -\frac{\kappa_2}{2}\delta a_2, \\ \delta\dot{b}_1 &= -\mathrm{i}[\omega_{b,1}\delta b_1-g_1(\alpha_1^*\delta a_1+\alpha_1\delta a_1^\dagger-\alpha_2^*\delta a_2-\alpha_2\delta a_2^\dagger)] \\ &\quad -\frac{\gamma_1}{2}\delta b_1, \\ \delta\dot{b}_2 &= -\mathrm{i}[\omega_{b,2}\delta b_2-g_2\alpha_2^*\delta a_2-g_2\alpha_2\delta a_2^\dagger]-\frac{\gamma_2}{2}\delta b_2. \end{aligned} \tag{A6}$$

Here, Eq. (A5) is the set of linear steady-state equations for cavity fields and resonators.

Acknowledgements

Project supported by the National Natural Science Foundation of China (Grant Nos. 61822114, 12074330, and 62071412).

References

[1] Klitzing K V, Dorda G and Pepper M 1980 *Phys. Rev. Lett.* **45** 494
[2] Haldane F D M 1988 *Phys. Rev. Lett.* **61** 2015
[3] Kane C L and Mele E J 2005 *Phys. Rev. Lett.* **95** 226801
[4] Bernevig B A, Hughes T L and Zhang S C 2006 *Science* **314** 1757
[5] Fu L 2011 *Phys. Rev. Lett.* **106** 106802
[6] Bansil A, Lin H and Das T 2016 *Rev. Mod. Phys.* **88** 021004
[7] Leykam D, Bliokh K Y, Huang C, Chong Y D and Nori F 2017 *Phys. Rev. Lett.* **118** 040401
[8] Li L, Yang C and Chen S 2015 *Europhys. Lett.* **112** 10004
[9] Niu Y, Chung S B, Hsu C H, Mandal I, Raghu S and Chakravarty S 2012 *Phys. Rev. B* **85** 035110
[10] Liu H F, Su Z X and Zhang Z Q 2020 *Chin. Phys. B* **29** 050502
[11] Zhang G and Song Z 2015 *Phys. Rev. Lett.* **115** 177204

[12] Kunst F K, Edvardsson E, Budich J C and Bergholtz E J 2018 *Phys. Rev. Lett.* **121** 026808
[13] Yao S and Wang Z 2018 *Phys. Rev. Lett.* **121** 086803
[14] Yao S, Song F and Wang Z 2018 *Phys. Rev. Lett.* **121** 136802
[15] Shen H, Zhen B and Fu L 2018 *Phys. Rev. Lett.* **120** 146402
[16] Jiang H, Yang C and Chen S 2018 *Phys. Rev. A* **98** 052116
[17] Wang H Y, Liu W M 2020 *Chin. Phys. B* **29** 047301
[18] Xu Z H, Li L H and Chen S 2013 *Phys. Rev. Lett.* **110** 215301
[19] Xu Z H and Chen S 2013 *Phys. Rev. B* **88** 045110
[20] Zhu S L, Wang Z D, Chan Y H and Duan L M 2013 *Phys. Rev. Lett.* **110** 075303
[21] Yan P, Lin R, Chen H, Zhang H, Liu A, Yang H and Ruan S 2014 *IEEE Photon. Technol. Lett.* **27** 264
[22] Gao L, Zhu T, Huang W and Luo Z 2015 *IEEE Photon. J.* **7** 1
[23] Ke S, Zhao D, Liu J, Liu Q, Liao Q, Wang B and Lu P 2019 *Opt. Express* **27** 13858
[24] Cui W X, Xing Y, Qi L, Han X, Liu S T, Zhang S and Wang H F 2020 *Opt. Express* **28** 37026
[25] Longhi S 2013 *Opt. Lett.* **38** 3716
[26] Blanco-Redond A, Andonegui I, Collins M J, Harari G, Lumer Y, Rechtsman M C, Eggleton B J and Segev M 2016 *Phys. Rev. Lett.* **116** 163901
[27] Liu Y C, Xiao Y F, Luan X and Wong C W 2013 *Phys. Rev. Lett.* **110** 153606
[28] Bai C H, Wang D Y, Zhang S, Liu S and Wang H F 2019 *Photonics Res.* **7** 1229
[29] Dobrindt J M, Wilson-Rae I and Kippenberg T J 2008 *Phys. Rev. Lett.* **101** 263602
[30] Vitali D, Gigan S, Ferreira A, Bohm H, Tombesi P, Guerreiro A, Vedral V, Zeilinger A and Aspelmeyer M 2007 *Phys. Rev. Lett.* **98** 030405
[31] Ghobadi R, Kumar S, Pepper B, Bouwmeester D, Lvovsky A and Simon C 2014 *Phys. Rev. Lett.* **112** 080503
[32] Purdy T P, Yu P L, Peterson R, Kampel N and Regal C 2013 *Phys. Rev. X* **3** 031012
[33] Nunnenkamp A, Børkje K, Harris J and Girvin S 2010 *Phys. Rev. A* **82** 021806
[34] Bai C H, Wang D Y, Zhang S and Wang H F 2019 *Sci. China Phys. Mech. Astron* **62** 970311
[35] Hasan M Z and Kane C L 2010 *Rev. Mod. Phys.* **82** 3045
[36] Qi X L and Zhang S C 2011 *Rev. Mod. Phys.* **83** 1057
[37] Aidelsburger M, Atala M, Lohse M, Barreiro J T, Paredes B and Bloch I 2013 *Phys. Rev. Lett.* **111** 185301
[38] Jing J, Ma Y Y and Zhang Q Y 2020 *Chin. Phys. B* **29** 080303
[39] Miyake H, Siviloglou G A, Kennedy C J, Burton W C and Ketterle W 2013 *Phys. Rev. Lett.* **111** 185302
[40] Kraus Y E, Lahini Y, Ringel Z, Verbin M and Zilberberg O 2012 *Phys. Rev. Lett.* **109** 106402
[41] Rechtsman M C, Zeuner J M, Plotnik Y, Lumer Y, Podolsky D, Dreiso F W, Nolte S, Segev M and Szameit A 2013 *Nature* **496** 196
[42] Zeuner J M, Rechtsman M C, Plotnik Y, Lumer Y, Nolte S, Rudner M S, Segev M and Szameit A 2015 *Phys. Rev. Lett.* **115** 040402
[43] Atala M, Aidelsburger M, Barreiro J T, Abanin D, Kitagawa T, Demler E and Bloch I 2013 *Nat. Phys.* **9** 795
[44] Jotzu G, Messer M, Desbuquois R, Lebrat M, Uehlinger T, Greif D and Esslinger T 2014 *Nature* **515** 237
[45] Li T, Duca L, Reitter M, Grusdt F, Demler E, Endres M, Schleier-Smith M, Bloch I and Schneider U 2016 *Science* **352** 1094
[46] Cui W X, Xing Y, Qi L, Han X, Liu S T, Zhang S and Wang H F 2020 *Laser Physics Letters* **17** 055206
[47] Leder M, Grossert C, Sitta L, Genske M, Rosch A and Weitz M 2016 *Nat. Commun.* **7** 13112
[48] Meier E J, An F A and Gadway B 2016 *Nat. Commun.* **7** 13986
[49] Yang Z, Gao F, Shi X, Lin X, Gao Z, Chong Y and Zhang B 2015 *Phys. Rev. Lett.* **114** 114301
[50] Li Y, Liu Y N and Zhang X 2020 *Chin. Phys. B* **29** 106301
[51] Roque T F, Peano V, Yevtushenko O M and Marquardt F 2017 *New J. Phys* **19** 013006
[52] Qi L, Xing Y, Wang H F, Zhu A D and Zhang S 2017 *Opt. Express* **25** 17948
[53] Raeisi S and Marquardt F 2020 *Phys. Rev. A* **101** 023814
[54] Qi L, Wang G L, Liu S T, Zhang S and Wang H F 2021 *Front. Phys.* **16** 12503
[55] Tsindlekht M, Golosovsky M, Chayet H and Davidov D 1994 *Appl. Phys. Lett.* **65** 2875
[56] Qi L, Xing Y, Liu S T, Zhang S and Wang H F 2020 *Phys. Rev. A* **101** 052325
[57] Farace A and Giovannetti V 2012 *Phys. Rev. A* **86** 013820
[58] Xu Z H, Zhang R, Chen S, Fu L B and Zhang Y B 2020 *Phys. Rev. A* **101** 013635